



## Hydrogen embrittlement of a torsion bar in a military aircraft

F. Leyx

*Università degli Studi di Roma "La Sapienza" (Italy)*

*leyx@hotmail.it*

F. Bagnoli, L. Allegrucci, F. Dolce, M. Bernabei

*Aeronautica Militare, Centro Sperimentale Volo - Reparto Chimico (Italy)*

---

**ABSTRACT.** The torsion bar of the emergency braking system of a military aircraft, a forged block of a maraging low-carbon steel, was found fractured during an in-service inspection. Visual examination of the bar showed several defects associated to the missing and blistering of finishing on both external and internal walls. Further examinations using a Field Emission Scanning Electron Microscopy (FESEM) as well as the X-ray Energy Dispersive Spectroscopy (X-EDS) and metallographic microscope showed pits in the protective finish from which started inter-granular corrosion. FESEM observation also revealed grains disbonding, in according to a hydrogen embrittlement phenomenon. Finite Element Analysis (FEA) also performed to evaluate stress distribution pointed out the orthogonality between the main stresses direction and the helical fracture.

Considering all the evidences, it was possible to ascribe the torsion bar failure to the hydrogen embrittlement. The pits, acting as raisers, just accelerated the failure mechanism.

In addition, it was suggested to intensify visual inspections, by checking of the finishing and eventually to replace the bars when defects are found.

**SOMMARIO.** La barra di torsione del sistema di frenaggio d'emergenza di un aereo militare, costituita da un unico blocco di acciaio martensitico invecchiato, è stata trovata rotta durante un'ispezione programmata. L'esame visivo ha evidenziato numerosi punti in cui il rivestimento superficiale era assente o rigonfiato. Ulteriori indagini condotte al FESEM, equipaggiato di EDS, e al microscopio metallografico hanno rilevato la presenza di pits corrosivi nel rivestimento protettivo. L'esame al FESEM ha anche permesso di rilevare scollamento dei grani tipico dei fenomeni di infragilimento da idrogeno. È stata condotta un'analisi agli elementi finiti per valutare la distribuzione degli sforzi, questa ha evidenziato ortogonalità tra gli sforzi principali e la superficie di rottura elicoidale.

Considerando tutte le evidenze, è stato possibile attribuire la rottura della barra di torsione all'infragilimento da idrogeno. I pits corrosivi hanno agito da concentratori degli sforzi, accelerando il meccanismo di frattura.

**KEYWORDS.** Failure analysis; Finite element analysis; Hydrogen embrittlement; Maraging steel; Torsion bar

---

### INTRODUCTION

The emergency braking system, located in the aircraft's tail (see the assembly in Fig. 1), guarantees the plane stop by catching with a hook a barrier cable located on the runway ground.

---

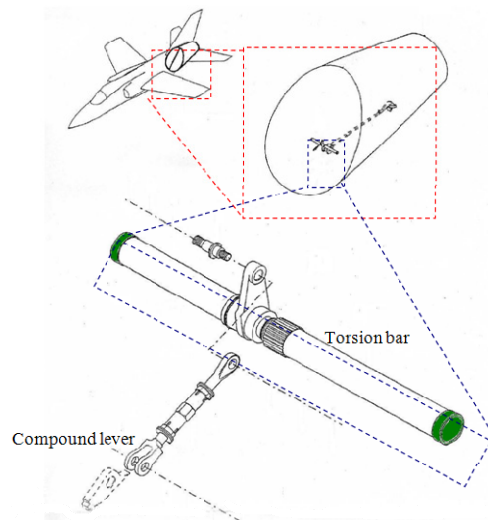


Figure 1: Torsion bar assembling scheme.

The hook is extracted by a compound lever actuated by a torsion bar pre-charged and locked during every pre-flight setup. The bar is unlocked by the pilot during landing in case of need. Pre-charging operation stores in the torsion bar elastic energy, thus making the component under continuous stress charge. A helical fracture was found on the torsion bar during a pre-flight setup. The bar is manufactured from a forged block of a maraging steel 18Ni(250) type, treated with a phosphatising process to guarantee the right adhesion of the protective coating. The failure investigation described in this paper was carried out by means of visual inspection, material characterization (namely, chemical and metallographic analyses, hardness measurements) and analysis of the fracture surface using FESEM and X-EDS. FEA was also performed to evaluate stress distribution in the bar. The results showed an anomalous hydrogen content in the material, thus determining an embrittlement of the bar. Corrosion pits, especially located on the external wall in length of about 270  $\mu\text{m}$  and due to the damaged finishing, accelerated the failure mechanism. In addition, FEA showed the orthogonality between the main stresses direction and the observed helical fracture, together with the low stress status if compared with the breaking load revealed by hardness measurements ( $\sigma_r = 176 \text{ kg/mm}^2$ ). In fact, near the fracture zone can be noted an increase of the main stresses values, but the maximum value is fairly lower than the yield point. Into the model it is also possible to see the orthogonality between the main stress directions and the initial fracture plane.

Following this investigation, it was recommended to check all the torsion bars installed and eventually remove all those having finishing defects of the external wall. It was also suggested to reduce the scheduled inspection intervals in order to verify the integrity of the finishing.

#### *Investigation equipment*

Visual examination was carried out by means of eye and using a Leica MZ12<sub>5</sub> optical microscope as well as fractography was made using a LEO Supra 35 FESEM equipped with a INCAx-Sight Oxford Instruments X-EDS. Microstructural examination was made using a Reichert Jung MeF<sub>3</sub> metallographic microscope, whereas a Perkin Elmer Optima 2100 DV ICP Optical Emission Spectroscopy was used for determining the chemical composition of the forged. The hardness measurements were carried out with A200 Hardness Rockwell Tester Officine Galileo equipped with a diamond indenter employed in the form of pyramid at 120° subjected to a load of 100 kg. The full load was also applied for 30 seconds, according to the Rockwell standard test method. Hydrogen quantity measurements were led within a LECO RH-402 hydrogen analyzer, while FEA was performed with ANSYS Mechanical v.11.

## RESULTS

#### *Visual examination*

**T**orsion bar consists of two concentric tubes connected at the extremities by two annuluses (see Fig. 2). In particular, the external one is partitioned in two pieces: the first one is 27 cm long and ends with a locknut at its free extremity, the second one, 20 cm long, ends with a lug bolt at which is connected the compound lever.

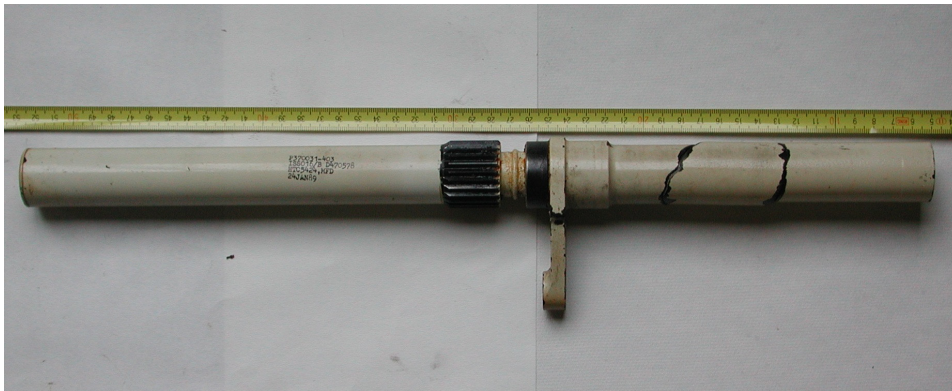


Figure 2: Torsion bar.

Visual examination revealed the presence of an helical fracture on the external tube ending with the lug bolt (see Fig. 3). The fracture is positioned about in the middle of tube length and covers almost 30% of its extension. In addition, spots where the finishing is removed or blistered were observed (see Fig. 4).



Figure 3: Helical fracture.

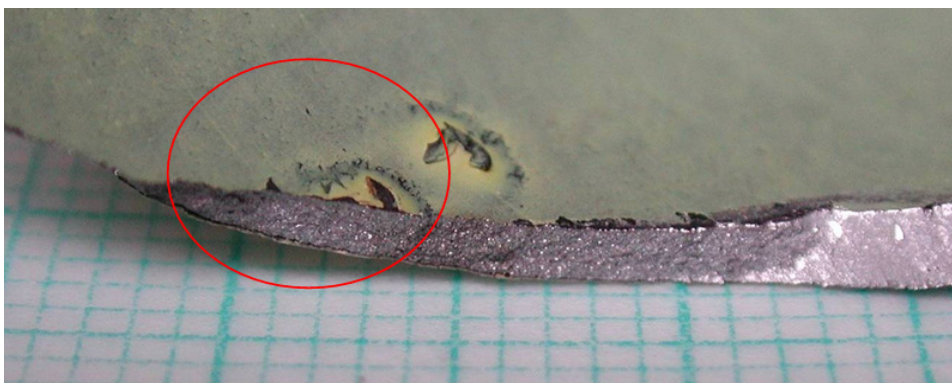


Figure 4: Blistering.

It is possible to notice three different planes of fracture: the central one is parallel to the radius and fine-grained, other two are oriented at  $\pm 45^\circ$  respect the radius and appears smooth and shining probably generated by a ductile overcharge fail. The central surface represents just the 5% of whole fracture surface and the external surface are perfectly symmetrical.

*Microstructural examination*

FESEM examination of the central fracture surface was carried out in order to determinate the failure mechanism. It is possible to identify three morphologic zones (A, B and C, see Fig. 5).

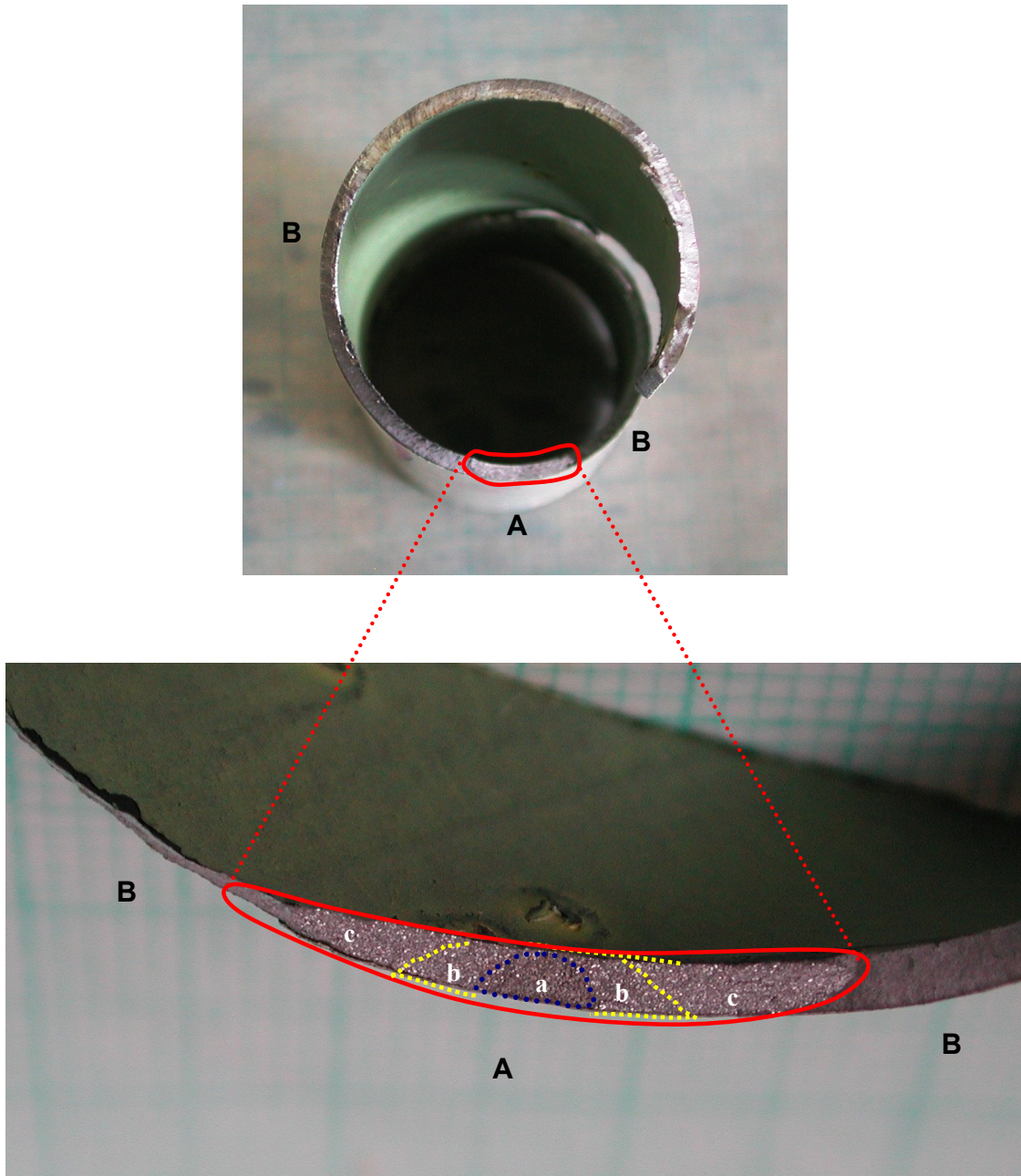


Figure 5: Morphologic zones.

The “A” zone is half elliptic shaped with the major axis about 3 mm long and the minor one extending for about 1 mm (Fig. 6).

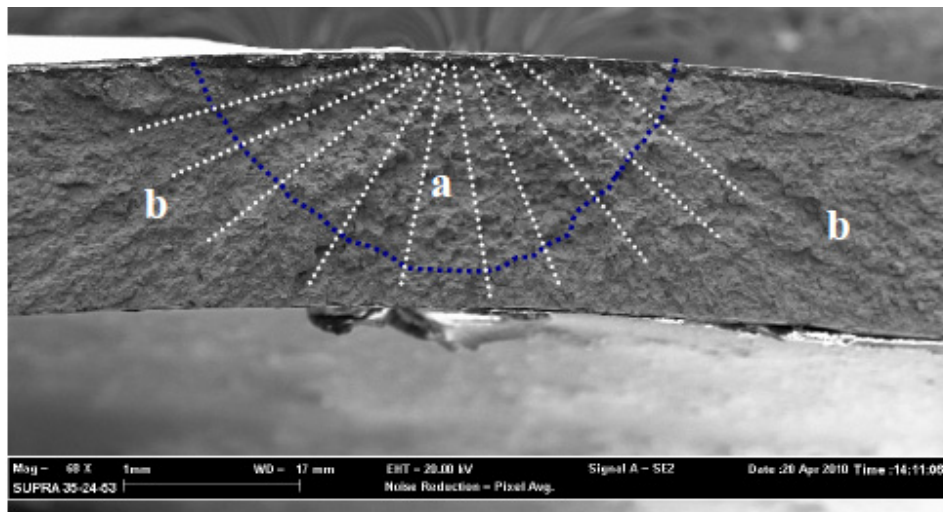


Figure 6: "A" zone.

Next to the external finishing can be observed a phosphate coating about 30  $\mu\text{m}$  deep; in addition on finishing were found several pits from 50 to 300  $\mu\text{m}$  wide (Fig. 7).

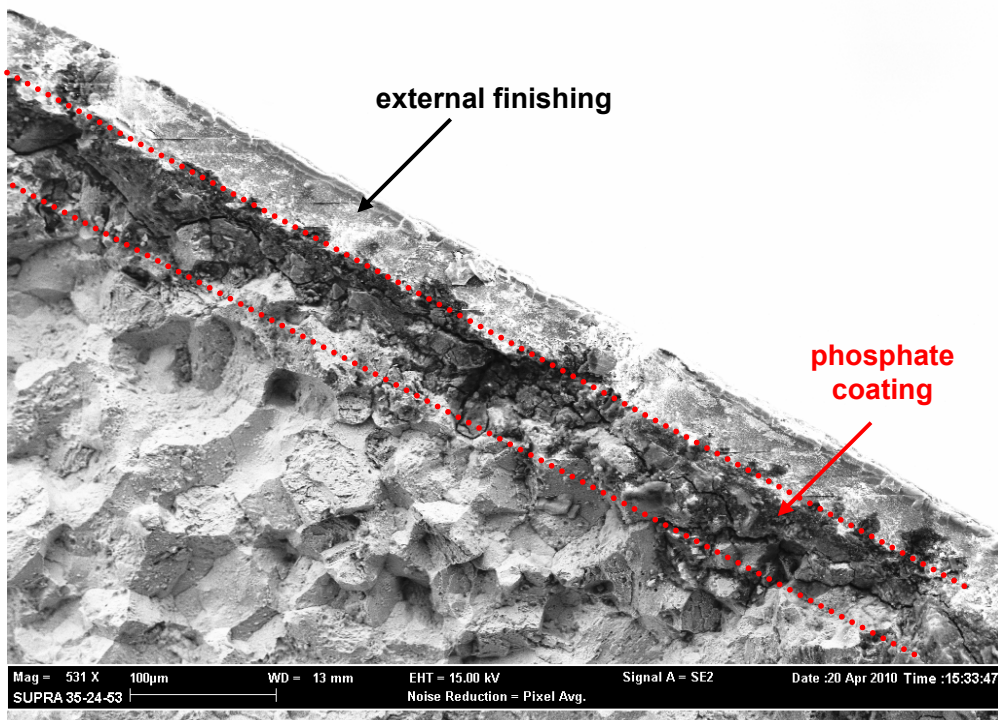


Figure 7: Morphologic zones.

Increased magnifications confirm the intergranularity of fracture. Grains result like disbonded with "hair lines" (see Fig 8), as high hydrogen inclusion fracture appears. Corrosion products were not found.

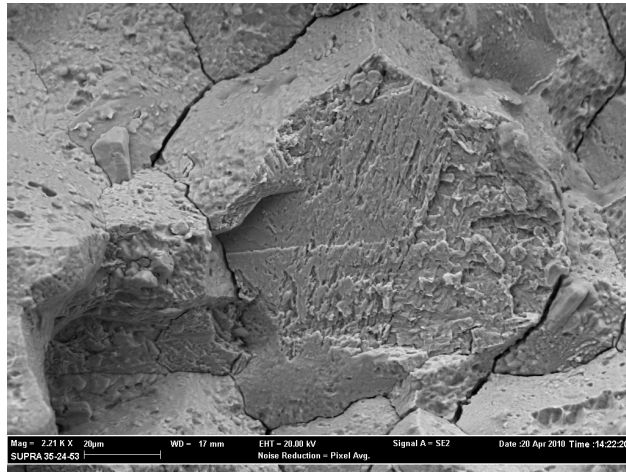


Figure 8: Grains disbanding.

“B” zone is 6 mm extended and is characterized by cleavage planes what means that a fragile fracture has occurred (see Fig. 9).

The remaining part of fracture surface, named as “C” zone, presents dimples due to a ductile overcharge fail (see Fig. 10).

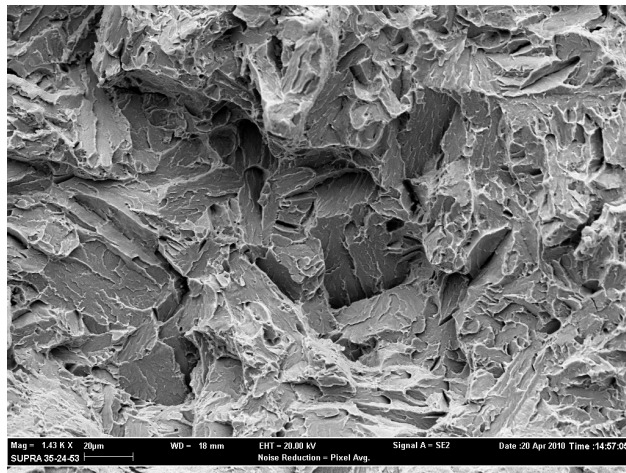


Figure 9: Cleavage.

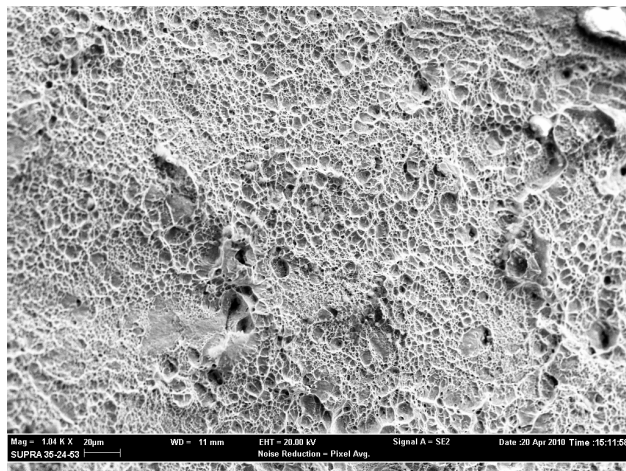


Figure 10: Dimples.



### *Metallography*

Metallographic examination was led on a cross section of the fracture surface next to the initiation point.

The core shows a typical low carbon maraging steel microstructure (see Fig. 11). A 75  $\mu\text{m}$  finishing, which consists of three different layers, is applied on a 30  $\mu\text{m}$  phosphate coating (see Fig. 12). Both, phosphate coating and finishing, are defective or absent in several spots.

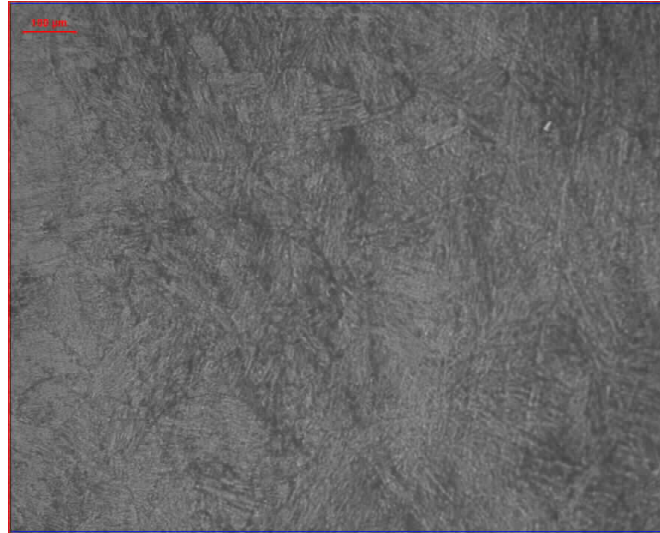


Figure 11: Core microstructure.

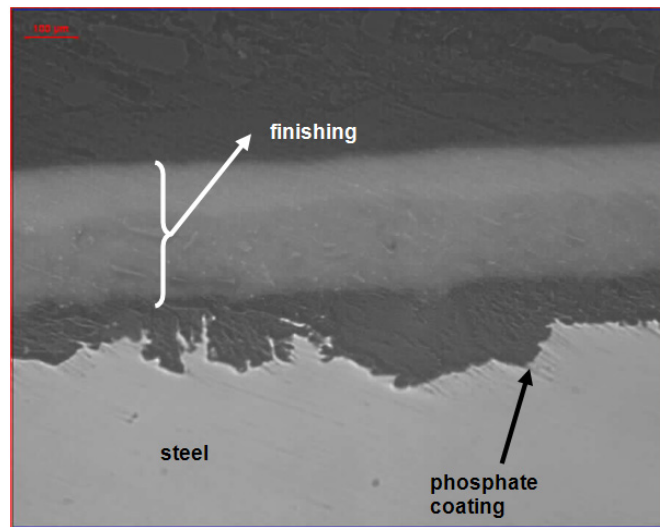


Figure 12: Finishing and phosphate coating

Operating a progressive ablation, once reached the initiation point it was possible to reveal a 270  $\mu\text{m}$  wide corrosion pit just below the external finishing (see Fig. 13). No secondary cracks were found.

### *Chemical analysis*

Quantitative analysis has been led within XRF technique scanning elements from fluorine to americium after sample grinding. In Tab. 1 are shown analysis results. Composition matches with a maraging steel type 18Ni(250).

Elements	Fe	Ni	Co	Mo	Ti	Si	Al	Mn	Cr
% weight	base	17.8	7.8	4.8	0.6	0.1	0.1	0.09	0.07

Table 1

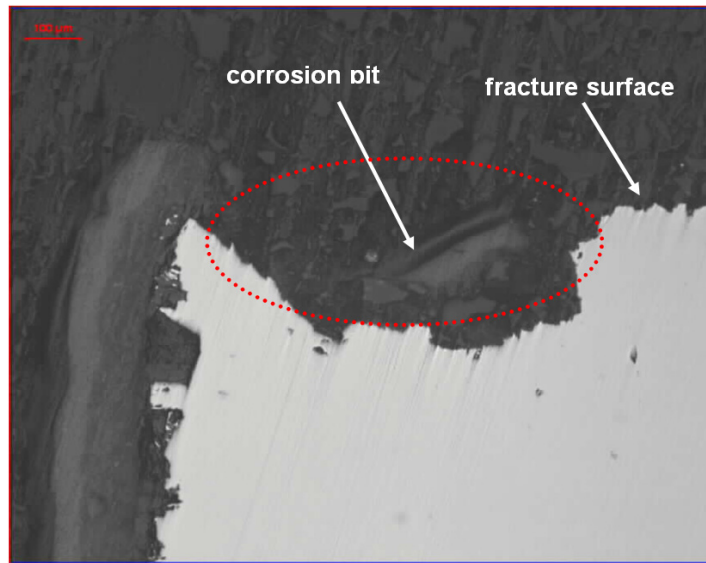


Figure 13: Corrosion pit.

#### *Hydrogen quantity determination*

Hydrogen quantity measurements were led by a LECO RH-402 hydrogen analyzer, four samples were taken in spots far from crack or cutting operations. After phosphate coating and finishing removal, it was obtained an average value of 3 ppm. Same analysis led on other two samples containing phosphate coating residues showed an average value of 6.9 ppm, instead of an allowed one of 2 ppm.

#### *Hardness measurements*

Hardness measurements were carried out on a polished sample in accordance with the Rockwell standard method. The section next to the lug bolt was measured to be 51 HRC ( $\sigma = 2.5$ ) corresponding to a 176 kg/mm<sup>2</sup> breaking load. This value is proper of an aged martensitic steel.

#### *FEA*

To identify the stress distribution on the torsion bar related with in-service condition of full up hook, a FEA was performed (Fig. 14) using a linear formulation.

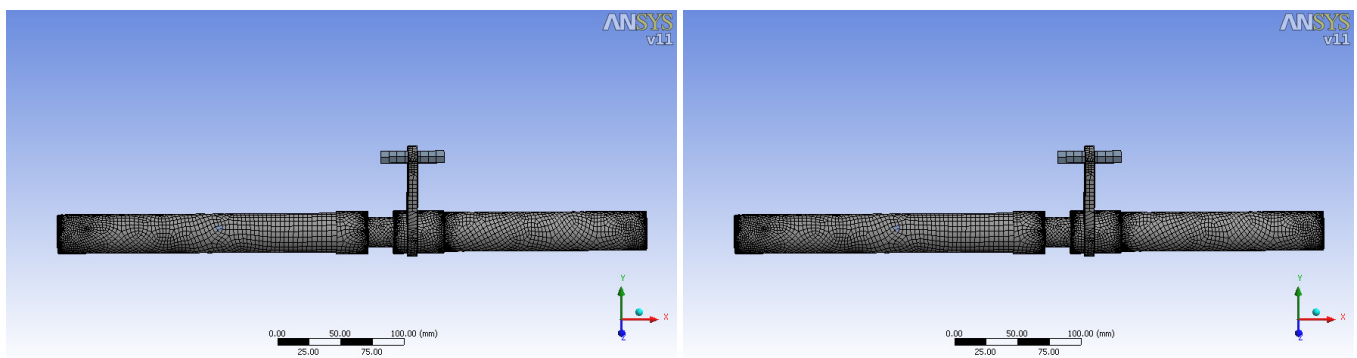


Figure 14: Mesh.

It was assumed the locknut as a fixed end (Fig. 15 - A) and only rotation around the main axis was allowed to the lug bolt end (Fig. 15 - B). To the lever connected to the lug bolt was assigned a displacement of 1 mm (Fig. 15 - C), a value probably quite lower than the real one generated during pre-charging operation.

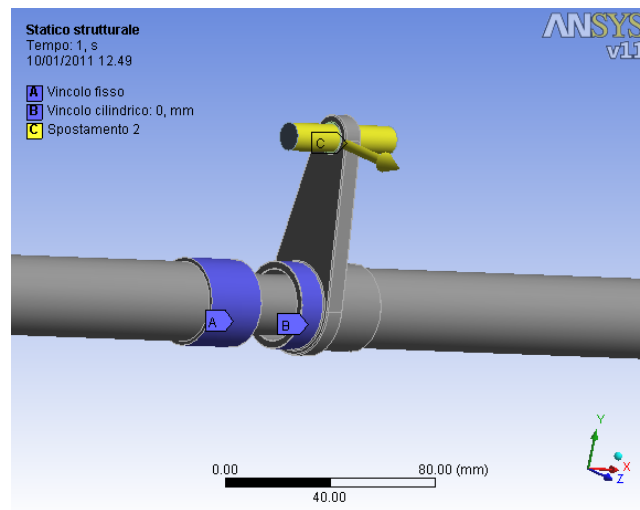


Figure 15: Constraints and displacements.

A Von Mises stresses increase was revealed near the fracture zone on both tubes (Fig. 16), in particular the maximum was located on the internal one.

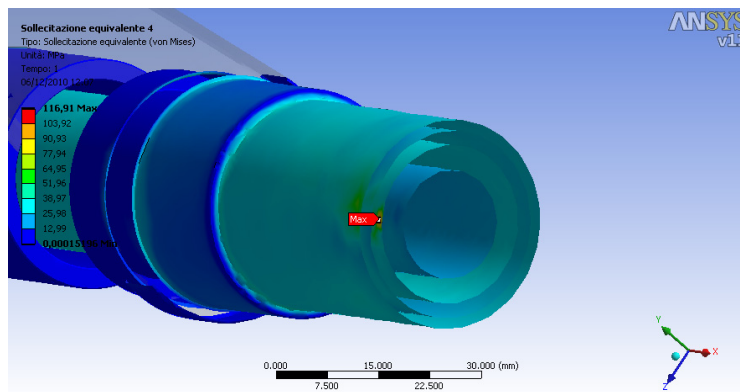


Figure 16: Von Mises stresses.

The stress values are not very high, much lower than the yield point (MPa), as largely expected with an applied displacement of 1 mm. It was pointed out the orthogonality between the main stresses direction and the helical fracture (Fig. 17).

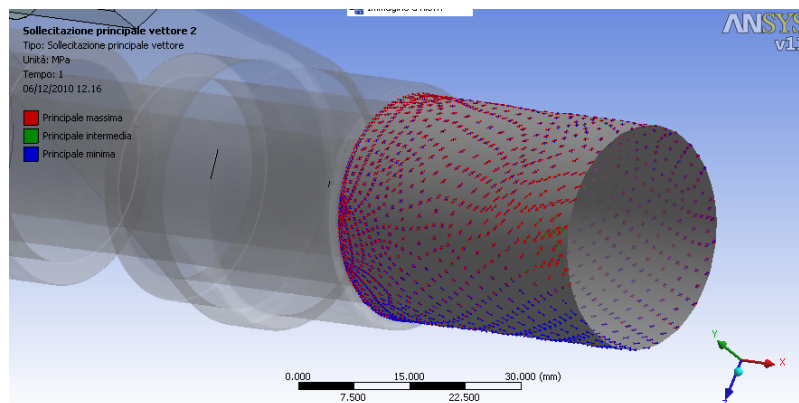


Figure 17: Main stresses vectors.



## ANALYSIS OF THE RESULTS

All evidence lead to ascribe the failure to a hydrogen embrittlement phenomenon. FESEM analysis showed intergranular fracture together to grain disbonding and hair lines, characteristic evidences of a brittle fracture. The microstructure as well as the hardness measurements tests were found satisfactory and in agreement with the original requirements. Metallographic exam revealed several finishing defects and corrosion pits, the biggest one located on the brittle fracture surface; moreover was detected a phosphate coating on the bar surface. FEA pointed out low stress values and orthogonality between main stresses direction and helical fracture.

A hydrogen embrittlement phenomenon acted on the torsion bar, but low stress value was not enough to lead to a failure. The 300  $\mu\text{m}$  corrosion pit found on the fracture surface worked as a stress raiser originating a brittle fracture surface, orthogonal to the main stress direction, on the external tube. Due to the reduced section, the fracture propagated as ductile.

## CONCLUSIONS

The investigation evidenced a hydrogen embrittlement failure of the torsion bar which was promoted by a corrosion pit on the external surface. Other similar pits were found on the bar surface, probably generated by a inadequate washing and drying after the phosphatation operation.

## REFERENCES

- [1] G. Oddone, Guida alla Interpretazione delle Caratteristiche Morfologiche delle Superfici di Frattura al Microscopio Elettronico a Scansione, Ragnò M. Editore, Roma (1981).
- [2] T. Poormina, J. Navak, A. N. Shetty, *Int. J. Electrochem. Sci.*, 5 (2010) 56.
- [3] A. Venugopal Reddy, *Aeronautical and Engineering Component Failures*, CRC Press LLC, 2000 N.W. Corporate Blvd., Boca Raton, Florida 33431, (2004).
- [4] *Enciclopedia degli Idrocarburi, Controllo della Corrosione e Scelta dei Materiali*, 5(9)2.
- [5] *ASM HandBook, Surface Cleaning, Finishing and Coating*, 5 (1992).
- [6] *ASM HandBook, Properties and Selection: Irons, Steels, and High-Performance Alloys*, 1 (1990) 222.
- [7] *Ibidem*, 797.
- [8] *Ibidem*, 799.
- [9] UNI EN ISO 4042:2003 – Elementi di Collegamento – Rivestimenti Elettrolitici.